Nonlinear Numerical Evaluation of Dynamic Behavior of an Asphaltic Concrete Core Rockfill Dam (A Case Study)

A. Akhtarpour[1] and A. Khodaii[2]

1. PhD. Student, Department of Civil and Environmental Engineering, Amirkabir University of Technology, Tehran, I.R. Iran, email: A_akhtarpur@aut.ac.ir
2. Associate Professor, Department of Civil and Environmental Engineering, Amirkabir University of Technology, Tehran, I.R. Iran

Keywords:
Dynamic behavior;
Nonlinear analysis;
Asphaltic concrete
core dam;
High seismic hazard

ABSTRACT

Nonlinear numerical analyses have been performed for the highest dam with asphalt concrete core in Iran (Shur River Dam) under seismic forces. The dam has 85 meters height and is under construction in an area with high earthquake hazard with MDE equal to 0.8g. Different stages of construction and impounding were analyzed using the hyperbolic model with Finite Difference Method. Nonlinear dynamic analyses were performed to investigate asphaltic core behavior under earthquake loading. The results show that earthquake shock can lead to developing some small cracks and increasing permeability of asphalt in the upper part of the core. Maximum vertical deformations occur near the crest and at the lower part of the upstream slope but would not be sufficient to cause loss of storage under normal operating conditions. Also deformation of asphalt core is completely dependent on the shell deformation and the thin wall core can not affect the general behavior of the dam. During the dynamic loading, different displacements between the thin core and transition layers are observed.

1. Introduction

1.1. Overview

Asphaltic concrete has been used for 50 years as an impervious interior core wall in hydraulic structures such as embankment dams [1-2]. Significantly important engineering properties of the asphaltic concrete used in hydraulic structures are workability during pouring and compaction, impermeability, flexibility and ductility to avoid cracking as a result of unfavorable filed stress and deformation conditions. In the regions with cold and rainy weather, construction of this kind of dam is easier and more economical than earth core dams. Monitoring of these dams has indicated their good behavior during construction and operation for many years [1-3]. However, most of the dams have been constructed in regions with low or moderate earthquake hazard and there is not any publication on actual dam behavior under sever earthquakes,

therefore, behavior of asphaltic concrete as impervious water barriers in high seismic hazard areas needs more attention and exploration [4-6].

In this study, the data from Shur dam with the height of 85*m* (Highest *ACRD* dam in Iran) which is under construction was selected as a case study. The results from numerical analyses show the response of this kind of core under static and dynamic loading.

1.2. Previous Numerical Studies

Valstad et al [7] analyzed the Storvatn dam located in Norway using a Newmark Approach. Their studies indicated that shearing off of the thin core near the crest may have occurred under severe shaking.

Hoeg [1] presented the results of Storvatn dam and showed that relatively large shear strains may

occur in the top of the core if dam slopes are very steep. However, he concluded that in general rockfill dams with asphaltic concrete core have a favorable seismic protection.

Meintjes and Jones [8] analyzed the Ceres dam located in south Africa using Newmark method. The predicted behavior of the dam was satisfactory.

Gurdil [9] performed seismic analysis of the Kopru dam located in Turkey. His analysis was based on the equivalent linear method. He concluded that some cracking may occur in the core, near the crest level. However, the self healing behavior of asphaltic concrete can solve this problem.

Ghanooni and Mahin-Roosta [6] performed dynamic analyses on a typical 115m high asphaltic concrete core rockfill dam. They concluded that in nonlinear analysis, the top section of the core experiences small tensile stresses which are less than asphalt material strength.

Salemi and Baziar [4] performed some numerical and experimental tests for Meyjaran dam in Iran with a height of 60m. They concluded that the asphalt concrete core behaves safely, even under very severe earthquake.

Feizi-Khankandi et al [10] performed a 2D nonlinear analysis on a 125m typical asphaltic concrete core rockfill dam. The results of the study show the appropriate response of the dam during and after an earthquake.

2. Shur River Dam

Shur dam that is under construction in south of Kerman province, is the highest concrete core rockfill dam in Iran. It has a height of about 85 meters and is located in a *U* shaped long valley. The crest length of the dam is about 450m and the vertical asphaltic concrete core, as a watertight element, has 1.2m width at the bottom decreasing to 0.6m on the top, which is surrounded by filters (zones 2a) and transitions in upstream and downstream (zones 2b), see Figure (1). The seismicity of the region is very high with *MDE* equal to 0.8g [11].

3. Finite Difference Method

3.1. Overview

A two dimensional, plane strain, dynamic deformation analysis of the Shur River Dam was performed using a finite difference program and its built-in elasto-plastic model of Mohr-Coulomb. The model requires elastic properties, a yield locus, a plastic potential, and a flow rule which is non-associated to shear-flow but associated to tensile flow [12-13].

In order to model variations in properties of the embankment materials with effective stress, (i.e. friction angle and shear modulus in dynamic analysis), a number of functions were developed using software's built-in programming language, *FISH*. Also *FISH* has been used to introduce hyperbolic nonlinear model in static analysis.

3.2. Geometry and Ground Water Conditions

The simplified embankment model and the finite difference mesh (*FDM*) used in analysis is shown in Figure (2).
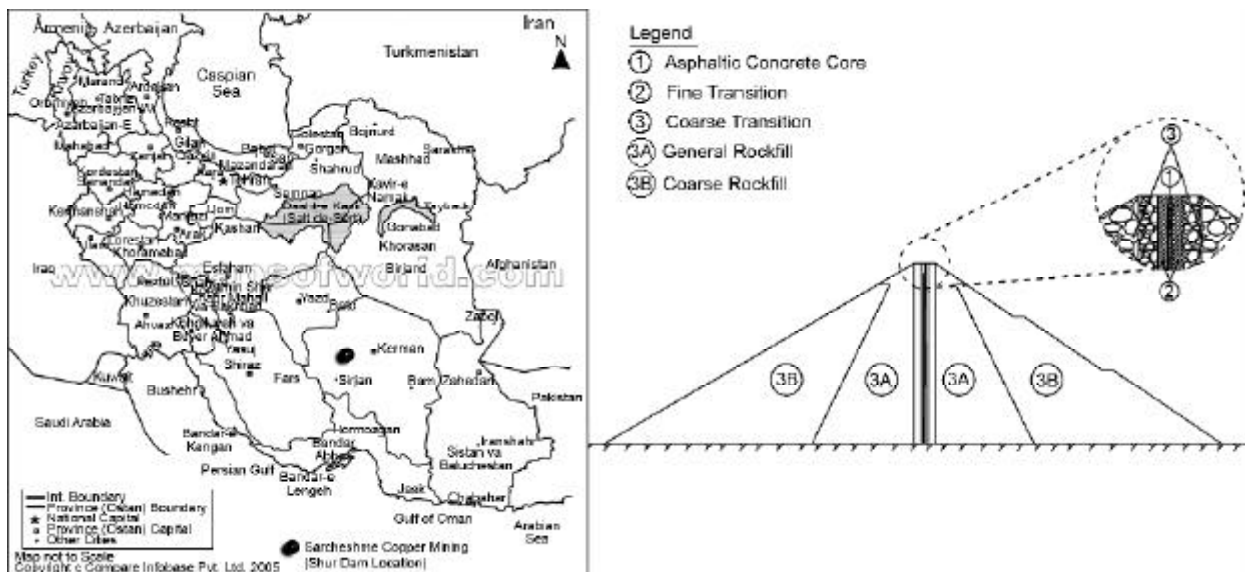

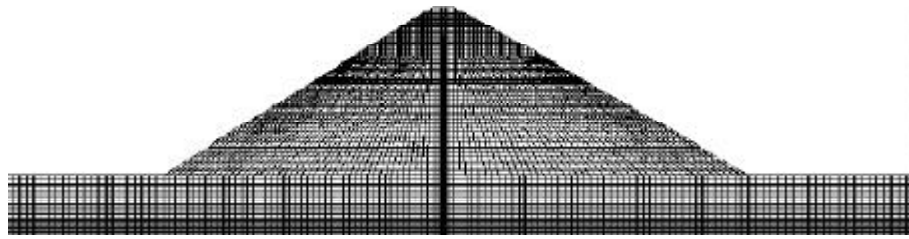**Figure 1.** Location and typical cross section of the Shur dam.

Figure 2. Finite difference grid generation.

Based upon the elastic properties of the materials used for the dam, the compression and shear wave speeds are [11]:

Cp = 753m/sec

Cs = 413m/sec

For accurate representation of wave transmission in the model, during dynamic analyses, the spatial element sizes were selected small enough to satisfy the following criteria expressed by Kuhlemeyer and Lysmer [14]:

$$Dl \leq \frac{\lambda}{10} \qquad (1)$$

Where λ is the wave length associated with the highest frequency component that contains appreciable energy and l is the length of element.

Ground water level at the end of construction stage was assumed to be at the base of the dam.

4. Static Analysis

Static analyses were carried out for various stages including end of construction and impounding. The hyperbolic model proposed by Duncan and Chang, [15] was used in these analyses. Tables (1&2) present the material properties used for numerical analyses.

4.1. End of Construction Stage

The analyses were performed using staged construction in 45 layers. Figures (3) and (4) show the vertical and horizontal displacements contours. The maximum settlement occurs inside the shell. The amount of maximum settlement is nearly 0.66*m*. Horizontal displacement has symmetric contours with the maximum of 21*cm*.

4.2. Impounding Stage

Water level increases to a height of 80*m* above

Table 1. Embankment material hyperbolic properties for rockfill and transitions [11].

Material	γ (Kg/m^3)	ki	Kb	Kur	n	m	Rf	C (Pa)	φ	$D\varphi$
Rockfill	2200	400	250	700	0.65	0.5	0.7	0	46	3
Transition	2150	200	150	400	0.4	0.5	0.7	0	38	4

Table 2. Embankment material Mohr-Coulomb properties for asphaltic concrete [11].

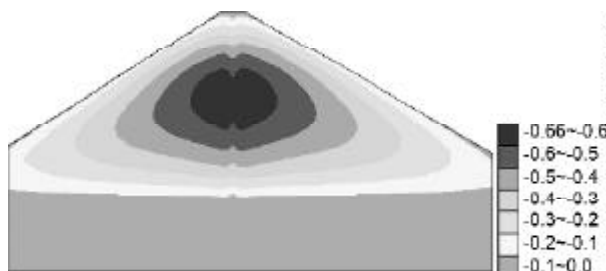| Material	γ (Kg/m^3)	E (MPa)	υ	C (kN/m^2)	φ	ψ
Asphalt	2420	150	0.49	360	18	0

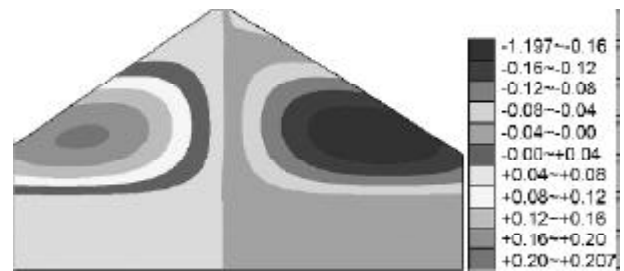**Figure 3.** Vertical displacements contours at the end of construction stage.

Figure 4. Horizontal displacements contours at the end of construction stage.

the base at three stages. During impounding, the hydrostatic force acts on the surface of the asphalt core because permeability of asphalt concrete is very low in comparison with the shell and transition materials. The adopted mobility coefficients and porosities for different materials are presented in Table (3).

A coupled flow and mechanical analysis has been done for modeling this stage. Figure (5) shows the predicted pore pressure contours after first filling to full supply level. The pattern of the pore pressure contours appears to be reasonable.

5. Dynamic Analysis

5.1. Input Ground Motion

ATC consulting engineers co. [11] has proposed three alternative ground motion records suitable for seismic analyses in their seismicity report on the Sarcheshmeh site.

From the two horizontal components of the acceleration-time histories, the most severe component was used for the modeling. All waves were normalized to *MDE* acceleration.

As can be seen in Figure (6), most of the energy in the input motions are at frequencies less than 15, 15 and 20*Hz* for Nahanni, Loma Prieta, and Cape Mendocino earthquakes, respectively.

Table 3. Embankment material hydraulic properties.

Material	Bedrock	Asphalt Core	Zones 2a/2b	Zone 3
Mobility Coefficient (m^2/Pa.s)	1×10^{-10}	1×10^{-15}	1×10^{-8}	1×10^{-6}
Permeability (m/s)	1×10^{-6}	1×10^{-11}	1×10^{-4}	1×10^{-2}

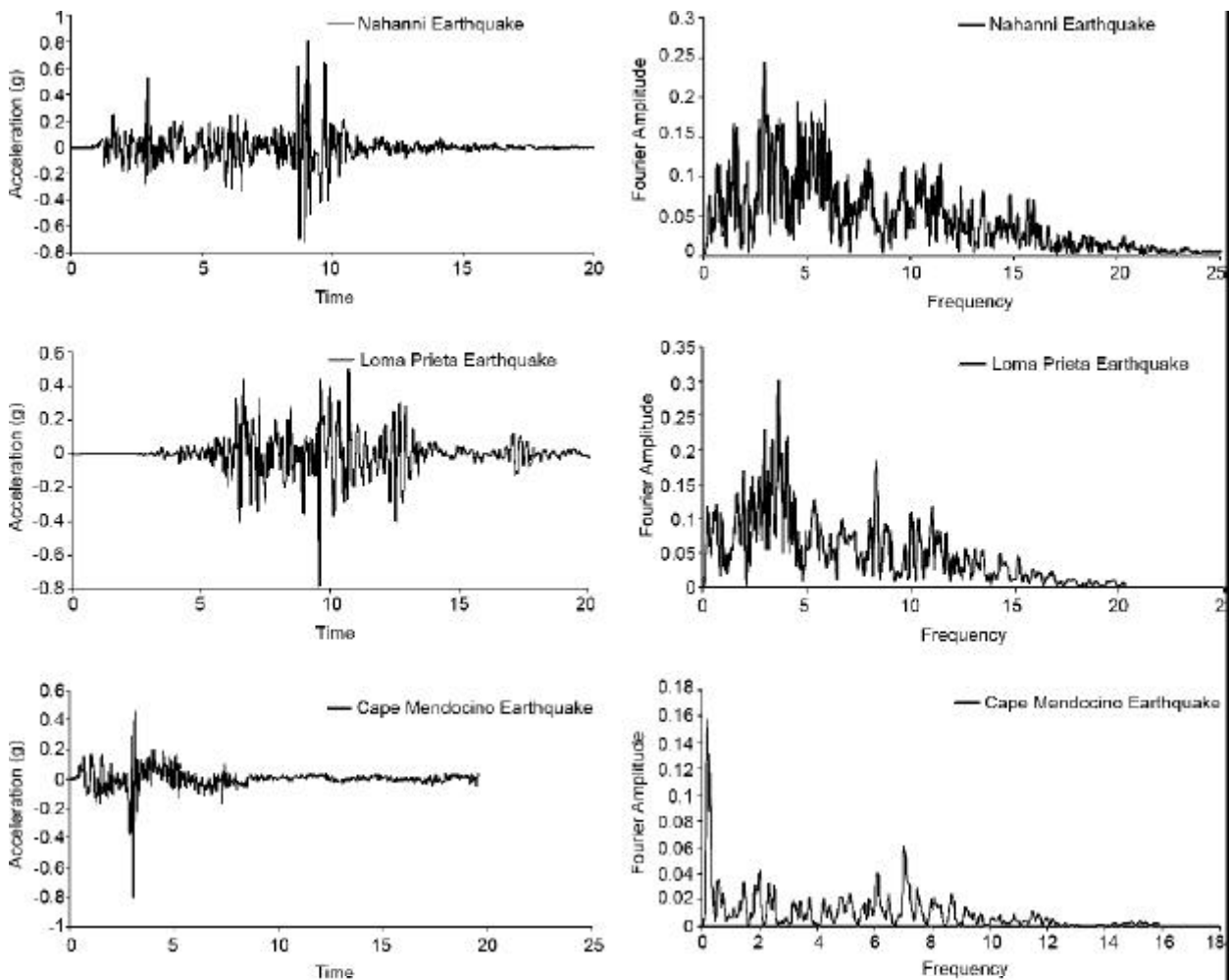**Figure 5.** Pore pressure contours after impounding.

Figure 6. Time history and frequency domain for Nahanni, Loma Prieta and Cape Mendocino earthquakes.

The seismic records were filtered to remove frequencies greater than the above frequencies. The filtering process was performed to limit the size of elements and to ensure accurate wave transmission.

After filtering was completed, the waves were corrected for a base line drift (i.e. continuing residual displacement after the motion has finished).

Finally the input motion to the model was applied as a shear stress boundary in order to establish quiet boundary conditions along the same boundary for the dynamic input as suggested by the software manual [12].

5.2. Material Properties

Stiffness and damping properties of the embankment materials used in the *FDM* analysis are summarized in Table (4), and are discussed in the following sections.

5.2.1. Rockfill Friction Angle

Douglas [16] after analyzing a large database of test results, developed Eq. (2) for shear strength of rockfills:

$$\sigma'_1 = RFI.\sigma'^{\alpha}_3 \tag{2}$$

The best estimation for α is 0.8726 and *RFI* is

a multiplier depending on initial porosity, angularity, maximum particle size, percent of fines and unconfined compressive strength. Lower bound, upper bound shear strength from all data and an adopted profile for Shur dam rockfill have been illustrated in Figure (7).

5.2.2. Shear Modulus

The small strain shear modulus, G_{max}, was determined using the methods described by Kramer [17] and the seismic refraction test results of the main dam foundation area [11]. G_{max} for the bedrock was calculated using the average shear wave velocity of 1050 *m/s* (measured in seismic refraction tests).

For zones 2 and 3, the G_{max} values were determined using the empirical relationship developed by Seed and Idriss [18] as follows:

$$G_{max} = 220 K_{2max}.\sigma_m^{0.5} \tag{3}$$

Where K_{2max} is the shear modulus coefficient and a function of relative density and soil types. For a good quality rockfill (i.e. zone 3), K_{2max} ranges from 120 at the surface to 180 at depths of 100 *m*. A value of 170 was adopted for zone 3 rockfill. For the transition zones (zone 2), a value of 90 was adopted [19].

Table 4. Stiffness and damping properties of embankment material.

Material	Poisson's Ratio	Shear Modulus G (MPa)	Initial Damping, %	Modulus Reduction and Damping Curve
Bedrock	0.23	2,700	1	Schnabel [20]
Asphalt Core	0.49	2,500	1	Nakamura et al [22]
Zone 2	0.3	*19.8 $\sigma_m^{0.5}$	1	Ishibashi and Zhang [21]
Zone 3	0.23	*37.4 $\sigma_m^{0.5}$	1	Ishibashi and Zhang [21]

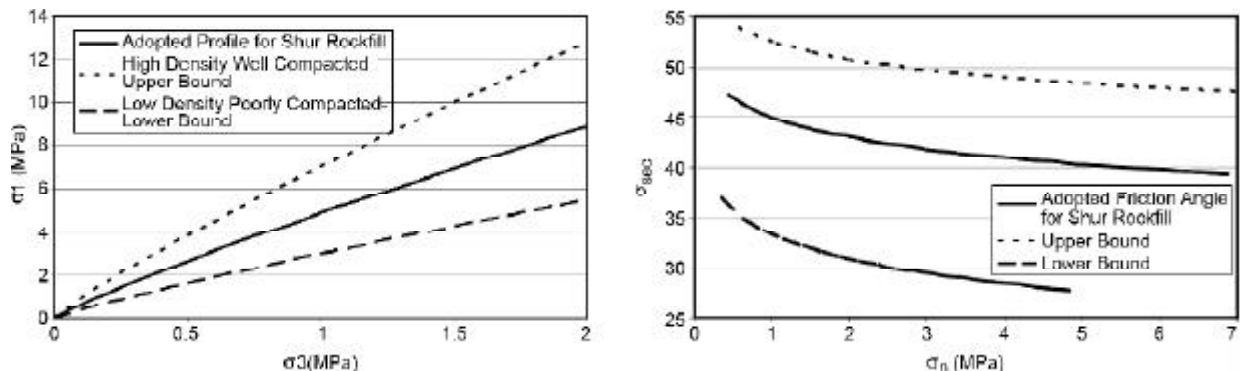* $\sigma_m^{0.5}$ is the mean effective stress.

Figure 7. Maximum principal stress vs. minimum principal stress (σ1 vs. σ3) and secant friction angle of rockfill vs normal stress (σ_{sec} vs. σ_n) (RFI = 4.8607) [16].

5.2.3. Damping

An initial damping ratio of 1% was assumed for all materials since the hysteretic damping shown in Figure (8) could not completely dampened the high frequency components of the dynamic inputs.

The adopted curves for bedrock are from Schnabel [20], and the curves for zones 2 and 3 are from Ishibashi and Zhang [21]. These curves were applied to the materials in the numerical model.
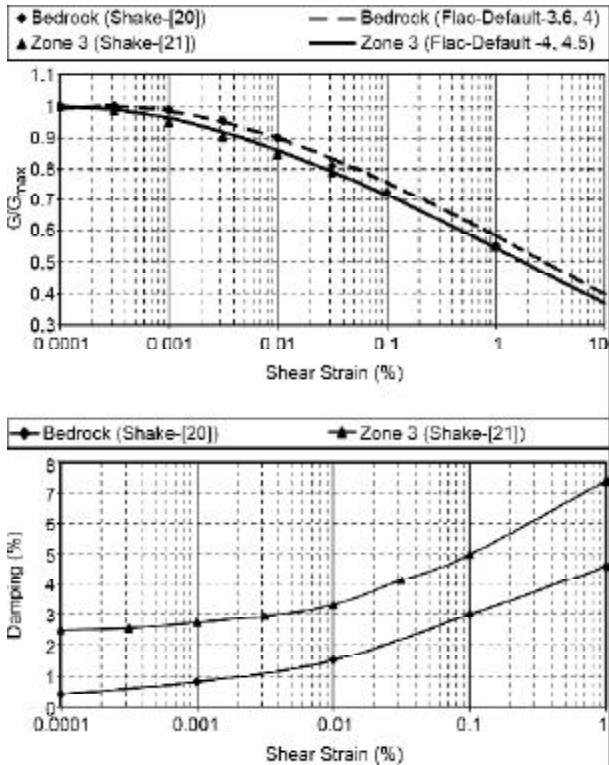

Figure 9. Reduction of shear modulus and damping ratio for asphaltic concrete core.

Figure 8. Variation in shear modulus and damping curves for zones 2 and 3 and bedrock.

This was carried out using the built-in default hysteretic model. The default hysteretic model is the *S* shaped curve of modulus versus logarithm of cyclic strain which has been represented by a third degree equation, with zero slopes at both small strain and large strain. This model requires two parameters, $L1$ and $L2$ which were obtained by curve fitting on the modulus reduction curves.

The adopted curves for asphaltic concrete are from Nakamura et al [22] using curve fitting method on default build-in hysteretic model. Figure (9) illustrates assumed curves for asphaltic core. As it can be seen, the built-in default hysteretic model has some deviation from Nakamura, specially in middle range of shear strains.
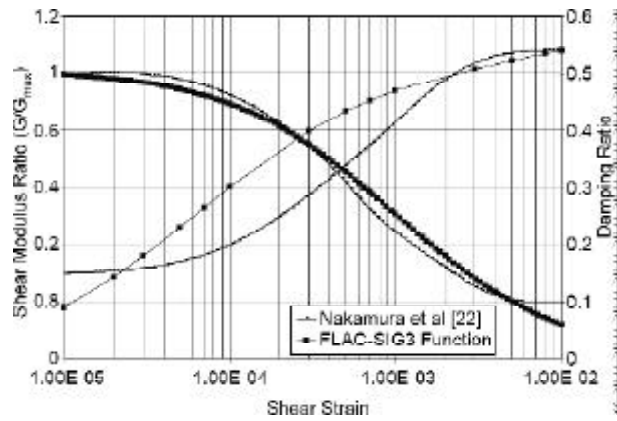
6. Analysis of Results

The general pattern of deformation as a result of seismic loading is shown in Figure (10). It is evident that the predicted pattern of deformation involves settlement and slumping of the rockfill on either side of the core, while the core generally remains upright, protruding from the slumped rockfill, with some lateral deformation. This is in agreement with typical behavior reported of this type of dams [4-6].
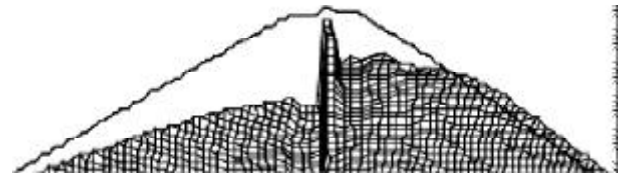

Figure 10. General pattern of deformation as a result of seismic loading (Magnification = 5.0 Max. Displacement = -2.15).

Crest acceleration and vertical deformation as a function of time are shown in Figures (11), (12) and (13), respectively, for each of the ground motion records analyzed. The results of the analyses are summarized in Table (5).

The predicted peak crest acceleration varies between 1.1g to 1.7g as compared to the input peak acceleration of 0.8g implying an amplification of 1.4 to 2.1. These ranges of amplifications are expected for rockfill embankment dams based on past experience reported in many studies [4-6].

It is evident that the predicted highest vertical displacement occurs at the embankment crest. These displacements attenuate rapidly with the depth and indicate no evidence of significant movements
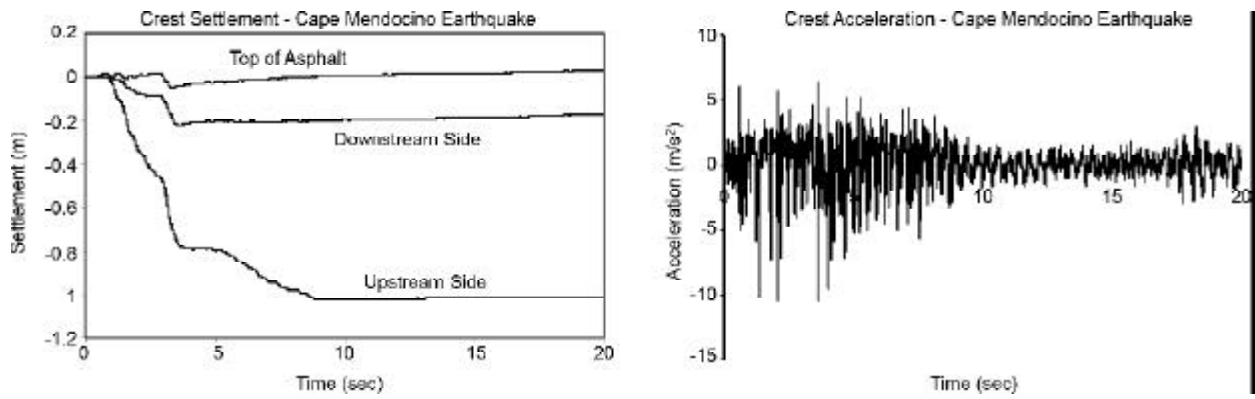
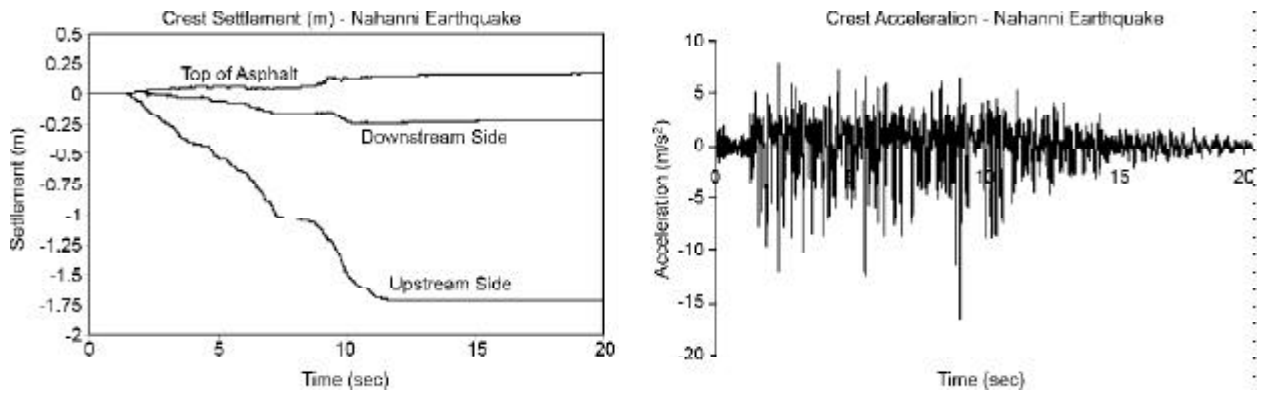**Figure 11.** Crest acceleration and vertical deformation as a function of time for Cape Mendocino earthquake.

Figure 12. Crest acceleration and vertical deformation as a function of time for Nahanni earthquake.
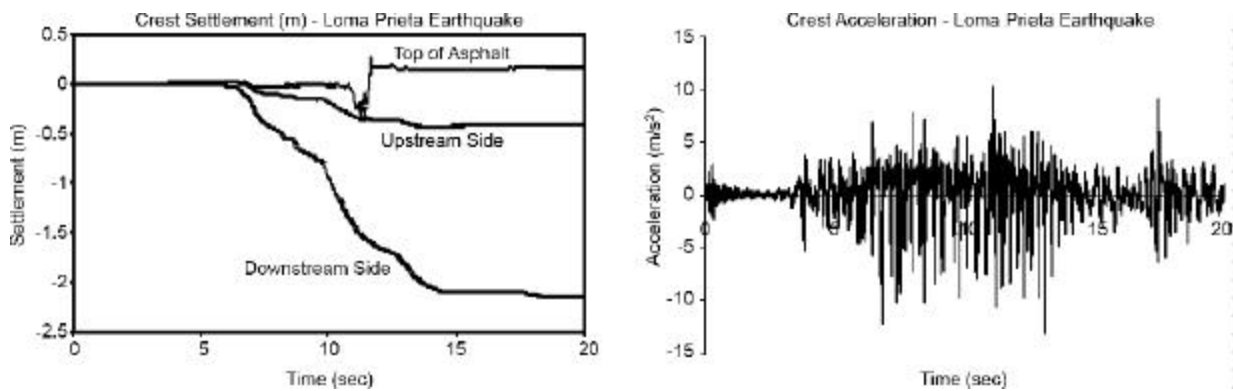

Figure 13. Crest acceleration and vertical deformation as a function of time for Loma Prieta earthquake.

Table 5. Summary of predicted displacements from FDM analysis.

Earthquake	Predicted Peak Crest Acceleration (g)	Predicted Crest Settlement (m)			Predicted Core Horizontal Relative[1] Displaceme nt (m)
		U/S	Core	D/S	
Loma Prieta	1.34	**-2.15**	+0.17	-0.40	-1.79
Cape Mendocino	1.1	**-1.01**[2]	+0.03	-0.17	-0.82[3]
Nahanni	1.68	**-1.71**	+0.17	-0.22	-1.12

1. Negative horizontal displacements indicates movement in the downstream direction and vice versa
2. Negative vertical displacement indicates settlement and vice versa
3. Relative to model base

of concern. The maximum crest settlement resulted from the Loma Prieta ground motion record with a vertical displacement of 2.15m, see Figure (13). Later studies by authors using Newmark approach utilizing quake/w and slope/w software resulted in upstream crest deformation equal to 2.25, 1.68 and 0.83 meter for each of ground motion records respectively that are in a good agreement with this study [23].

The results of the *FDM* analysis indicate that the maximum deformations will occur near the crest and at the lower part of the upstream slope. The magnitude of the estimated deformations appears to be large but would not be sufficient to cause loss of storage under normal operating conditions. The predicted maximum vertical deformation of 2.15m does not exceed the embankment freeboard of 4.0m. Shear strains and lateral displacement in center of the embankment core resulting from each of the ground motion records are shown in Figure (14).

It can be seen that the predicted maximum relative lateral deformation of the core is approximately 1.78m at the embankment crest, resulting from the Loma Prieta ground motion record.

While the predicted maximum horizontal deformation of 1.78m does exceed the width of the asphalt core, 0.6m, this deformation is associated with slumping in the upstream face of the embankment. Furthermore, the analysis suggests that the core has sufficient ductility to deform and prevent complete disassociation of any part of the core.

At the levels of shear strains observed, plastic deformation of the core is expected, and cracking of the core may occur in the upper 15 meter of the dam.

Remaining shear strains varies between 4~7% at 15 meter below crest level to more than 12% at normal water level. Experimental studies shows that it can lead to developing some cracks and increasing permeability of asphaltic core [1] but water pressure is not enough to cause high concentrated seepage and leakage of the dam body.

7. Summary and Conclusions

❖ The results of the *FDM* analysis confirm that the critical embankment slope for seismic stability is the upstream slope.

❖ The maximum predicted deformation of the rockfill is a vertical deformation of 2.15m, determined using the *FDM* Software. Under normal operating conditions a minimum freeboard of 4.0m is provided between crest level and spillway level. Thus, deformations of this magnitude would not cause the storage to be breached and are considered to be acceptable.

❖ Deformations of asphalt core are completely dependent on the shell deformations and one meter thin wall core can not affect the general behavior of the dam.

❖ During the dynamic loading, different displacements between the thin core and transition layers are observed.
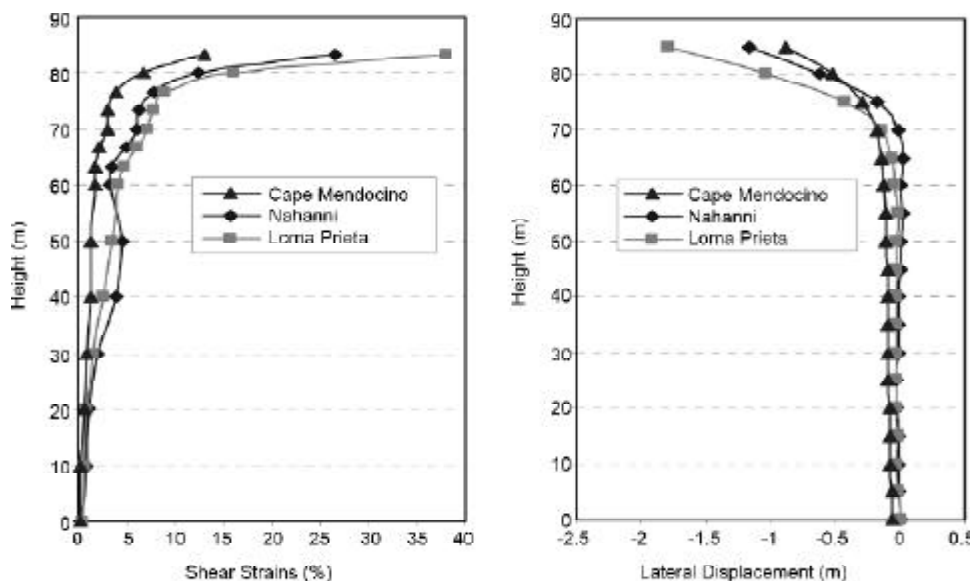
❖ Nonlinear analyses shows that the amount of

Figure 14. Shear strains and lateral displacement of asphaltic core after earthquake loading.

cyclic shear strain is very small inside the asphalt core in comparison with the filter and transition layers. Value of cyclic shear strain is relatively small in the thin core. This value in transition layers in either side of the core is very high and it means that these materials have reached their plastic mode.

❖ Based on the predicted deformation of the embankment core and estimated level of internal shear strain in the core material, complete disassociation of the embankment core is not to be expected but developing cracks and increasing permeability in higher part of core may have occurred. At this level water pressure is not enough to cause leakage and failure.

❖ Based on the numerical analysis, as presented in Figure (14), lateral displacements above 70 meters height increases rapidly, hence it seems that reduction in core thickness with the height of the dam, as considered in design, is not appropriate.

References

1. Hoeg, K. (1993). "Asphaltic Concrete Cores for Embankment Dams", Norwegian Geotechnical Institute of Technology, Oslo, Norway.

2. ICOLD Press, Bituminous Cores for Earth and Rockfill Dams (1982 and 1992). Bulletin 42 and 84.

3. Creegan, P. and Monismith, C. (1996). "Asphaltic Concrete Water Barriers for Embankment Dams", ASCE Press.

4. Salemi, Sh. and Baziar, M.H. (2003). "Dynamic Response Analysis of a Rockfill Dam with Asphalt-Concrete Core", *Proc. of Soil and Rock American Conference*, MIT, Boston.

5. Feizi-Khankandi, S., Mirghasemi, A.A., and Ghanooni, S. (2004). "Behavior of Asphaltic Concrete Core Rockfill Dams", *International Conference on Geotechnical Engineering* (ICGE), UAE.

6. Ghanooni, S. and Mahin Roosta, R. (2002). "Seismic Analysis and Design of Asphaltic Concrete Core Dams", *Journal of Hydropower and Dams*, **9**(6), 75-78.

7. Valstad, T., Selness, P.B., Nadim, F., and Aspen, B. (1991). "Seismic Response of a Rockfill Dam with an Asphaltic Concrete Core", *J. of Water Power and Dam Construction*, **43**, 1-6.

8. Meintjes, H.A.C. and Jones, G.A. (1999). "Dynamic Analysis of Ceres Dam", *Proceedings of the 12th Regional Conference for Africa on Soil Mechanics and Geotechnical Engineering*, Durban South Africa.

9. Gurdil, A.F. (1999). "Seismic Behaviour of an Asphaltic Concrete Core Dam," *1st Symposium on Dam Foundation*, Antalya, Turkey, 581-600.

10. Feizi-Khankandi, S., Mirghasemi, A.A., Ghalandarzadeh, A., and Hoeg, K. (2008). "2D Nonlinear Analysis of Asphaltic Concrete - Core Embankment Dams", *The 12th International Conference of International Association for Computer Methods and Advances in Geomechanics (IACMAG)*.

11. Design Report, "Shur River Dam", Australian Tailing Consultants, ATC (2008).

12. Itasca Consulting Group (1998). "Fast Lagrangian Ana-lysis of Continua", Minneapolis, Minnesota, USA.

13. Vermeer, P.A. and de Borst, R. (1984). "Non-Associated Plasticity for Soils, Concrete and Rock", Heron, **29**(3), 1-64, (Quoted by Itasca 1998).

14. Kuhlemeyer, R.L. and Lysmer, J. (1973). "Finite Element Method Accuracy for Wave Propagation Problems, *Journal of Soil Mechanics and Foundations, Div. ASCE*, **99**(SM5), 421-427.

15. Duncan, J.M. and Chang, Ch.-Y. (1970). "Members ASCE, 1970, Nonlinear Analysis of Stress and Strain in Soils", *J. Soil Mechanics and Foundation Engineering*, **96**(SM5), 1622-1651.

16. Douglas, K.J. (2002). "The Shear Strength of Rock Masses", Ph.D. Thesis, School of Civil and Environmental Engineering, Sydney Australia, Chapter 4.

17. Kramer, S.L. (1996). "Geotechnical Earthquake Engineering", Prentice-Hall International Series in Civil Engineering Mechanics, USA.

18. Seed, H.B. and Idriss, I.M. (1970). "Soil Moduli and Damping Factors for Dynamic Response Analyses", Report EERC 70-10, Earthquake Engineering Research Center, University of California, Berkeley, USA.

19. Seed, H.B., Wong, R.T., Idriss, I.M., and Tokimatsu, K. (1984). "Moduli and Damping Factors for Dynamic Analyses of Cohesionless Soils, *J. of Geotechnical Engineering*, **112**(11), 1016-1032.

20. Schnabel, P.B. (1973). "Effects of Local Geology and Distance from Source on Earthquake Ground Motions", Ph.D. Thesis, University of California, Berkeley, USA.

21. Ishibashi, I. and Zhang, X.J. (1993). "Unified Dynamic Shear Moduli and Damping Ratios of Sand and Clay", *Soils and Foundations*, **33**(1), 182-191.

22. Nakamura, Y., Okumura, T., Narita, K., and Ohne, Y. (2004). "Improvement of Impervious Asphalt Mixture for High Ductility Against Earthquake Excitation", *Proc. New Developments in Dam Engineering*, 647-656.

23. Akhtarpour, A., Khodaii, A., and Ebrahimi, A. (2009). "Evaluation of Dynamic Response of an Asphaltic Concrete Core Rockfill Dam Using Newmark Approach (A Case Study)", *Int. J. of Civil Engineering,* IAUST (Submitted).